Proceedings of the 21st ICSMGE, Vienna, Austria, 14 – 19 June 2026. Pistrol, Adam & Schweiger (eds.)
Published by: ÖGG, Austrian Society for Geomechanics, Salzburg, Austria, ISBN 978-3-9503898-4-5
https://doi.org/10.53243/ICSMGE2026-487

Effect of deep excavations on the construction site seismic demand during earthquake occurrence

Ilaria Esposito, Marco Valerio Nicotera, Gianpiero Russo
University of Napoli Federico II, Napoli, Italy, ilaria.esposito3@unina.it

Grigorios Tsinidis
University of Thessaly, Volos, Greece

ABSTRACT: Deep excavations in urban environment, mainly realized for the construction of metro stations, are often placed very close to existing above-ground buildings. The interaction in static conditions has been widely investigated, whereas in seismic conditions it is almost completely disregarded. This study starts from a case study, namely the San Pasquale station of Napoli Metro, that is excavated through different layers of sandy soils, with the water table being only 1 m below ground level and the Neapolitan yellow tuff constituting the bedrock of the site. To investigate the effects of the excavation and construction of this station on the nearby buildings, finite element models of the examined case have been developed, representing two scenarios. The first one refers to the excavation works phase, and it is calibrated to accurately reproduce the recorded response via monitoring instruments, installed on the buildings and inside the retaining structures of the station shaft, during the construction of the station. In this context the effects of stress-strain history experienced by the soil during the excavation process are accounted for in the subsequent seismic analysis phase. The second model represents a free field condition, since no excavation is simulated before the seismic analysis phase, and it is used as a benchmark for the first one. The results of the seismic analysis phase of the two models are compared and presented herein in terms of maximum acceleration at the ground level, and frequency content of the related time histories. Two main alignments are considered, parallel and orthogonal to the seismic input direction respectively, in order to highlight the modification of the seismic excitation at the ground level due to the metro station.
KEYWORDS: coupled seismic analysis, dynamic characterization, urban excavation.

1 INTRODUCTION

Excavation works are often carried out in the city centers to build car parks or metro stations. In this kind of work the main effort is generally made in trying to minimize their interaction with the surrounding buildings and underground existing infrastructures in static conditions (*i.e.*, settlements, displacements, induced strains and related stresses), while the interaction occurring during the design earthquake is not considered by current codes nor by practitioners. However, it is worth noticing that some literature contributions, especially for tunnels and box culverts (Youta-Mitra et al., 2007; Abate & Massimino, 2017; Wang et al., 2013; Sun et al., 2019) or natural cavities (Lee, 1984; Liang et al., 2012; Sica et al., 2014), have analyzed the problem of the modification of acceleration and displacement field around the discontinuity highlighting the influence of the distance of the control point from the excavation, the direction of the applied input motion and the frequency content of the input signal. The actual execution of this kind of work, though, (excavations even more than tunnels) is strongly dependent on many specific factors such as geometry, soil conditions, presence of water etc., which makes each job a case of its own. In this paper the information about the construction of a deep metro station realized in the city of Napoli is used as a starting point to build a tridimensional FEM model -only the excavation and its structures are reproduced, while no buildings are modelled-, firstly aimed at reproducing the field displacements at the end of the excavation and, then, at performing coupled dynamic analyses in time domain, using a non-linear constitutive model for the soil, to study the seismic effect of the shaft on the spatial distribution of accelerations at the ground level in the surroundings, along two alignments, parallel and orthogonal to the direction of the applied input. The results obtained allow to draw some conclusions of general applicability, given that some simplifications were assumed in the numerical model with respect to the real case.

2 THE CASE STUDY: SAN PASQUALE STATION

2.1 *Soil and stratigraphy*

The site interested by the excavation is placed next to the seaside and the ground surface is just a couple of meters above sea level. It was investigated with a campaign of geotechnical in-situ tests that was performed before the excavation began, including boreholes, seismic dilatometer tests (SDMT), cone penetration tests with pore pressure measurements (CPTu), standard penetration tests (SPT), cross hole (CH), Lugeon and Lefranc permeability tests. Based on the results of the campaign it was possible to reconstruct soil stratigraphy, schematically represented in Fig. 1, and to derive the properties useful for soil characterization in the numerical model (described in section 3). The water level in the excavated area typically fluctuates between 1 m and 2 m below the ground surface and can be considered approximately coincident with the ground level. The subsurface stratigraphy within the project area comprises a succession of sandy deposits, exhibiting variations in grading and relative density, overlying a bedrock formation of Neapolitan Yellow Tuff (NYT). Consistent with the depositional and post-depositional characteristics of volcanic pyroclastic materials (Russo et al., 2012), the tuff does not exhibit a planar surface; instead, the bedrock interface displays a markedly irregular and undulating morphology. As illustrated in Figure 1, the coloured rectangular boxes delineate the longitudinal profile of the planned station, which extends for approximately 85 m. Within the footprint of the station shaft, the elevation of the tuff ceiling varies significantly, occurring at depths between 32 m below ground level (bgl) in the shallower sectors and 45 m bgl in the deepest zones where the bedrock surface is depressed. This variability in the depth to bedrock results in pronounced heterogeneity in the thickness of the overlying sandy strata. In locations where the NYT is relatively shallow, the sandy cover is limited, whereas in other sectors, the increased depth of the bedrock is accompanied by

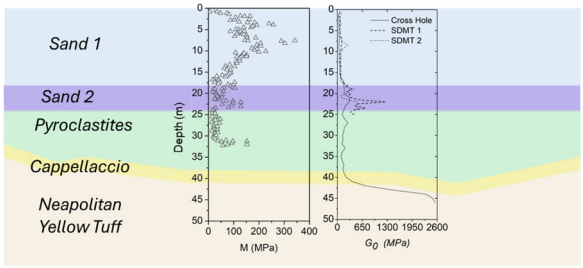

Figure 1. Soil stratigraphy of the site and main parameters derived from CH and SDMT tests.

substantially thicker uncemented overburden. While these stratigraphic complexities may exert a considerable influence on both design and analysis, the present investigation adopts a simplified representation of the subsurface conditions, with the objective of deriving conclusions of wider applicability.

2.2 *Execution of the work and monitoring plan*

The excavation has a rectangular plan (24x85.5 m^2) and a depth of 27 m (Fig. 2).

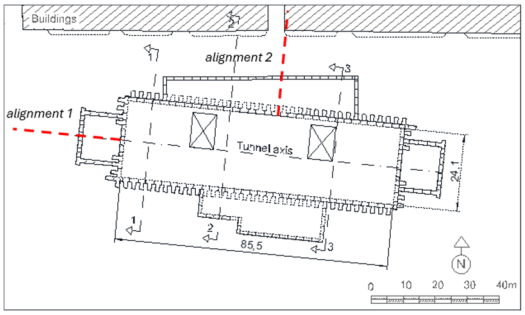

Figure 2. Plan view of the station.

The station's main shaft is enclosed by T-section reinforced concrete diaphragm walls. Each panel was obtained by partial overlap of two rectangular excavations extending to a depth of approximately 50 m to ensure substantial embedment within the Neapolitan Yellow Tuff (NYT). Such embedment was readily achieved owing to the relatively soft mechanical properties of the volcanic tuff. Further details on the construction technology, challenges in T-panel excavation, and the resulting ground displacements are reported in L'Amante et al. (2012), Russo et al. (2019). Due to the presence of valuable historical structures in the vicinity – most notably the Villa Pignatelli (18th century)– stringent deformation control criteria were adopted. This requirement was addressed through a top-down construction procedure, involving the sequential execution of the following main geotechnical stages:

a. installation of all diaphragm walls;
b. formation of jet-grouting beneath the access shaft;
c. excavation of the main tunnel using a TBM;
d. staged excavation under preliminary groundwater lowering.
e. placement of a waterproof membrane at the shaft base;
f. casting of the bottom slab.
g. cessation of groundwater lowering;
h. partial removal of intermediate slabs and execution of finishing works.

The overall construction period was approximately four years, with major works carried out between July 2010 and 2014. Among the preliminary geotechnical works, dewatering tests with different layouts were performed to minimize the risk of unforeseen hydraulic behaviour during the main excavation. The top-down procedure made it possible to minimize the induced settlements on the buildings bordering it, whose facades are at a mean distance of 17 m (minimum of 12 m) from the edge of the pit. Inclinometers, benchmarks on buildings and sidewalks and piezometers allowed to control the induced effects during the works, which were negligible: the maximum displacements and settlements being in the range 20-30 mm and the effect of the lowering of the water table below the bottom of the excavation was contained within the perimeter of the shaft.

3 FEM MODEL AND ANALYSES

3.1 *Numerical model*

The numerical model is built on FE software PLAXIS 3D 2024.2 (Bentley, 2024). The soil domain has a volume of 120×200×70 m^3 and the station shaft is located approximately in the middle of it. It is composed by 288×10^3 elements with average dimension equal to 3.9 m, with the mesh more refined in the softer soils (according to the prescriptions by Kuhlemeyer & Lysmer (1973), on the maximum dimensions of the elements for dynamic numerical analyses). The soil stratigraphy reproduces the sequence derived from the in-situ tests (Fig. 1). The marine sandy soils (Sand 1 and Sand 2) and the pyroclastic sandy soil (PYR) are reproduced in the numerical model with the Hardening Soil model with small strain stiffness (HSss) (Benz, 2007) particularly suitable for static analyses of excavations in sands and adaptable for dynamic analyses as well (Benz *et al.*, 2009); the linear elastic perfectly plastic Mohr-Coulomb (MC) model, with a Rayleigh damping equal to 1%, was used to simulate the behavior of Neapolitan yellow tuff (NYT) and the overlying *cappellaccio* (Cap), that is a thin layer of altered or weakly cemented tuff; the main properties assigned to the different soil layers – assumed as horizontal layers in the numerical model– are summarized in Tables 1 and 2 and have been established partly based on empirical correlations with field tests (L'Amante et al., 2012), partly on laboratory decay curves obtained on materials sampled on site (Fabozzi et al., 2017).

Table 1. Sandy soil properties

Soil	Depth	E^{ref}_{50}	E^{ref}_{ur}	G_0	ϕ	c
HSss	m bgl	MPa	MPa	MPa	°	kPa
Sand 1	0-18	37	120	91.5	38	1
Sand 2	18-24	15	45	170	38	1
Pyr	24-39	9.4	30	144	37.2	1

Table 2. Rock properties

Soil	Depth	E'_{ref}	ν'	ϕ'	c'
MC	m bgl	GPa	-	°	kPa
Cap	39-42	1.9	0.3	27	150
NYT	42-70	5.5	0.3	27	500

The interface between soil and structures have the same properties as the adjacent soil, with the strength properties reduced by a factor 0.67, for the sandy layers. For the interface between structures and tuff or *cappellaccio*, that are soft rocks, a new material was defined with the aim of reducing the cohesion to nearly zero value.

3.2 *Static stages of the analysis*

The RC structures of the station, consisting of 6 slabs 0.9 m thick, diaphragm walls and the internal lining (realized after the completion of the excavation), are modelled as linear elastic plates. Orthotropic stiffness properties were assigned to the plates representing diaphragm walls to replicate the effect of the t-shaped sections; they were activated during the first phase of calculation, without simulating the installation procedure. The

activation of the slabs is alternated with soil removal stages and lowering of the water level below the bottom of the excavation.

In the final stage of the analysis the water level is restored to its initial level throughout the entire domain, which simulates the pump shutdown, and the foundation of the pit is activated.

Despite some simplifications assumed in the model with respect to the real case (horizontal stratigraphy, access shaft not modeled), the results of the static stages in terms of water flow, shape and entity of settlements are comparable to those registered in site. Thus, it is possible to assume that the state of stress of the soil is near to that acting in situ at the end of the construction.

3.3 *Dynamic analyses*

The 3D model described in the previous section was used to perform and compare two scenarios: the first is the soil domain with the shaft where all the static stages were simulated, as already described in section 3.2, the second, useful for comparison, is a free field analysis where only the stratigraphy was reproduced. The analyses are performed in undrained conditions.

3.3.1 *Selection of the input motions*

According to the Italian building code NTC 2018, to perform the dynamic analyses in time domain 7 spectrum-compatible accelerograms were selected for the site and subjected to a deconvolution procedure with the 1D linear equivalent code SPECTRA. The inputs underwent a baseline correction and a filtering procedure with a band-pass filter in the range 0.1-10 Hz with a Butterworth filter of 8th degree. The choice of the accelerograms to be used for the complete coupled dynamic analyses has been made based on the dynamic characterization of the system through a frequency sweep analysis: the system was solicited with a sinusoidal function in acceleration, with constant amplitude equal to 10^{-3} g, and frequency spanning from 0 to 10 Hz, with a rate of 0.1 Hz/s, and the first two eigen-frequencies resulted equal to 1.6 and 4.4 Hz. For space reasons, in the present paper the results are relative to only 006332xa signal, which, among the 7 selected, is the one with the highest peak acceleration, 0.18 g, and whose mean and peak frequencies are 2.6 Hz and 2.0 Hz respectively.

3.3.2 *Boundary conditions*

The analyses are performed ensuring one-dimensional propagation. The input motion was applied at the bottom of the model with a surface displacement, along x direction (parallel to the main plan dimension of the shaft), while it was verified that the accelerations in the other two directions are at least three orders of magnitude lower than those in x direction. Tied-node boundary conditions were imposed at the lateral boundaries in the direction in which the seismic input was applied (Zienkiewicz et al., 1989). The initial horizontal effective stress profile was applied with surface loads at the vertical boundaries perpendicular to the seismic input (y-z plan), and the constraints to horizontal displacements, active in static conditions, were removed.

4 RESULTS

The results presented in the following compare the two analyses described in section 3.3 to make some observations on the effect of the shaft on the distribution of acceleration around it. The quantities taken into consideration are peak ground acceleration and Fourier spectra of the acceleration time histories. Two alignments are considered: alignment 1, along the direction of application of the input, and alignment 2, along the direction orthogonal to it (see Fig. 2). The sampling points are at increasing distances from each other moving away from the excavation. First, it was verified that the free field case actually behaved as free field, which is verifying that any location responded in the same way to the input. The comparisons for alignment 1 are represented in Fig. 3 in terms of maximum acceleration profiles (left) and corresponding Fourier amplitudes (right) in the range of frequencies of interest (0-5 Hz), based on the dynamic properties of the system discussed in section 3.3.1. It can be seen that the response is quite the same everywhere, except for some minor differences in the acceleration profiles in the sandy layers (maximum discrepancies of about 10%), especially in the first 10 m bgl, which can be due to the proximity to the lateral boundaries. Same considerations can be made about Fourier amplitudes, that overlap almost completely for all locations considered.

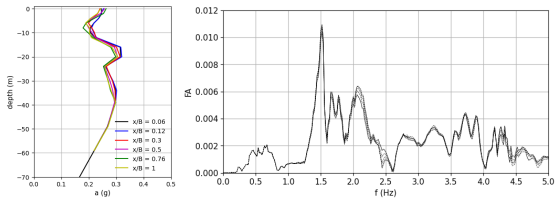

Figure 3. Left: acceleration profiles along different columns in free field conditions (alignment 1). Right: Fourier amplitudes

The ratios between the peak acceleration computed at the ground level in the excavation case with respect to the free field analysis are reported in Figs. 4 and 5 for the two above-mentioned alignments. The ratio is plotted as a function of a dimensionless parameter of distance d_{adim} defined as the ratio between the distance from the edge of the shaft along an alignment and the half dimension of the shaft itself in that direction. In both cases the influence of the excavation is well visible, with a clear reduction (about 25%) of peak acceleration close to the excavation edge, followed by an increase at higher distances that reaches a value of +50%.

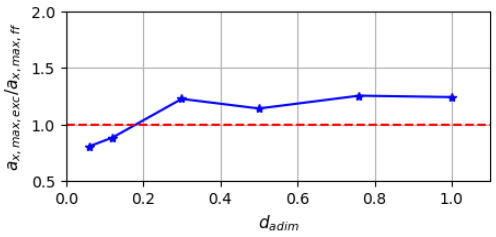

Figure 4. Peak ground acceleration increments (blue line) along alignment 1.

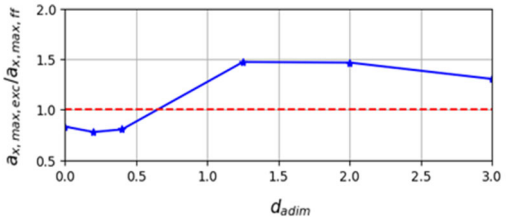

Figure 5. Peak ground acceleration increments (blue line) along alignment 2.

More information on the modification of the system response is given by the representation in frequency domain in Figs. 6 and 7, for alignment 1 and 2 respectively. The Fourier amplitudes computed from the acceleration time histories at the ground level are compared for the *excavation* and the *free field* cases.

A significant deamplification is registered in the *excavation* case in the first two locations closer to the pit, which confirms the results already discussed in terms of peak

acceleration. As d_{adim} increases, the Fourier amplitudes of the *excavation* case increase as well in both cases. It must be noticed, though, that despite the similar trend of peak ground accelerations, the frequency content along the two alignments is different. Along alignment 1 the amplitude associated with the peak at 2 Hz increases most, while the peak frequency of the free field case (1.6 Hz) is deamplified. Along alignment 2 (orthogonal to the input direction) the frequency content is still modified by the excavation but the frequency amplitude most sensitive to the increasing distance is at 1.6 Hz.

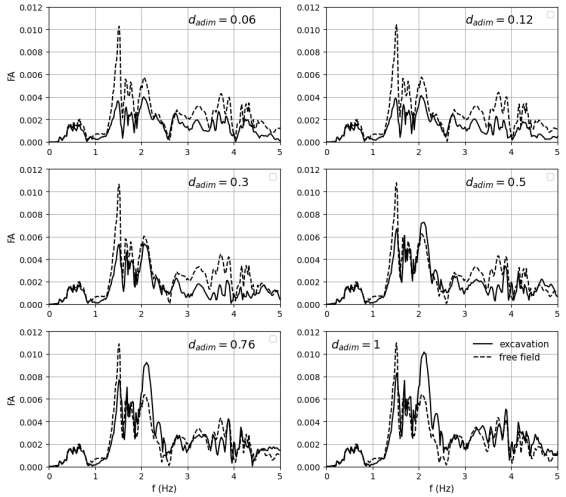

Figure 6. Fourier amplitudes at different distances from the shaft (see Fig. 2) along alignment 1: excavation (continuous line) vs free field (dashed line) comparison.

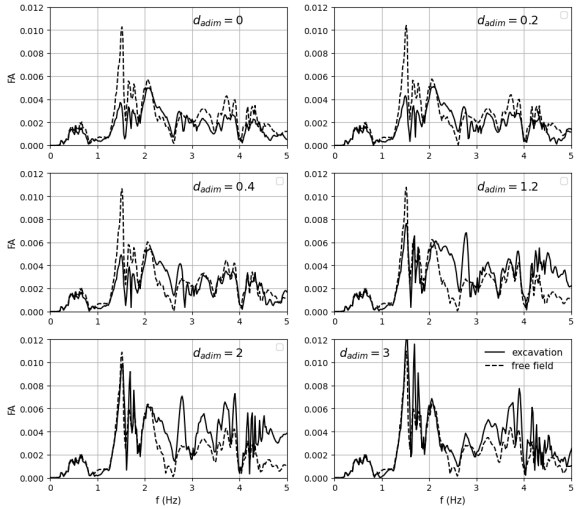

Figure 7. Fourier amplitudes at different distances from the shaft (see Fig. 2) along alignment 2: excavation (continuous line) vs free field (dashed line) comparison.

5 CONCLUSIONS

The modification of the site seismic demand around a deep metro station has been investigated in the paper using the finite element software PLAXIS 3D. The seismic hazard has been analysed by considering the procedure suggested by the national code NTC 2018 which in turn is derived by Eurocode 8 – Part 1 (EN 1998-1) for the site of the station which is located in the city of Napoli. Because of space constraints only the results relative to one out of the seven selected time histories have been reported. The full 3D dynamic analyses have been carried out using nonlinear soil model and taking as starting stage the last one simulating the static construction of the station. The main findings reported in the paper are as follows. First, significant modifications of the peak ground acceleration at the ground surface are computed as the resulting influence of the presence of the supported deep excavation with respect to a free field scenario. It is clearly shown that these modifications depend on the distance from the edge of the station and from the direction of the seismic input. Furthermore the Fourier spectra of acceleration time histories of several points at the ground surface clearly show that the distance from the edge also plays another role which is that of changing the frequency content and particularly the frequency corresponding to the highest amplitude.

6 ACKNOWLEDGMENTS

This study was partially funded by the European Union - NextGenerationEU_, in the framework of the _GRINS -Growing Resilient,INclusive and Sustainable_ project (MUR: GRINS PE00000018 – CUP E63C22002140007).

7 REFERENCES

Abate, G., & Massimino, M. R. 2017. Numerical modelling of the seismic response of a tunnel–soil–aboveground building system in Catania Italy. *Bulletin of Earthquake Engineering*, *15*, 469-491.

Bentley 2024. PLAXIS 3D 2024.2 – Reference Manual.

Benz T., Small-strain stiffness of soils and its numerical consequences, Ph.D. thesis, University of Stuttgart, 2007.

Benz, T., Schwab, R., & Vermeer, P. 2009. Small-strain stiffness in geotechnical analyses. *Bautechnik*, *86*S1, 16-27. doi.org/10.1002/bate.200910038

Fabozzi, S., Licata, V., Autuori, S., Bilotta, E., Russo, G., & Silvestri, F. 2017. Prediction of the seismic behavior of an underground railway station and a tunnel in Napoli Italy. *Underground Space*, *2*2, 88-105.

Kuhlemeyer, R. L., & Lysmer, J. 1973. Finite element method accuracy for wave propagation problems. *Journal of the soil mechanics and foundations division*, *9*95, 421-427.

L'Amante D., Flora A., Russo G., Viggiani C. 2012. Displacements induced by the installation of diaphragm panels. *Acta Geotech*, 73:203–218, doi: 10.1007/s11440-012-0164-9

Lee, V. W. 1984. Three-dimensional diffraction of plane P, SV & SH waves by a hemispherical alluvial valley. *International Journal of Soil Dynamics and Earthquake Engineering*, *3*3, 133-144.

Liang, J., Zhang, J., & Ba, Z. 2012. Amplification of in-plane seismic ground motion by group cavities in layered half-space I. *Earthquake Science*, *25*4, 275-285. doi.org/10.1007/s11589-012-0853-3

Russo G., Viggiani C., Viggiani G.M.B. 2012. Geotechnical design and construction issues for lines 1 and 6 of the Naples underground. *Geomechanics and Tunnelling,* 53: 300-311,

Russo, G., M. V. Nicotera, and S. Autuori. 2019. Three-Dimensional Performance of a Deep Excavation in Sand. *J. Geotech. Geoenv. Eng.* https://doi.org/10.1061/ascegt.1943-5606.0002037.

Sica, S., Dello Russo, A., Rotili, F., & Simonelli, A. L. 2014. Ground motion amplification due to shallow cavities in nonlinear soils. *Natural hazards*, *71*, 1913-1935.

Sun, Q., Dias, D., Guo, X., & Li, P. 2019. Numerical study on the effect of a subway station on the surface ground motion. *Computers and Geotechnics*, *111*, 243-254.

Wang, H. F., Lou, M. L., Chen, X., & Zhai, Y. M. 2013. Structure–soil–structure interaction between underground structure and ground structure. *Soil Dynamics and Earthquake Engineering*, *54*, 31-38.

Yiouta-Mitra, P., Kouretzis, G., Bouckovalas, G., & Sofianos, A. 2007. Effect of underground structures in earthquake resistant design of surface structures. In *Dynamic response and soil properties* pp. 1-10).